



# 1 The Lightning Differential Space Framework: Multiscale Analysis

# of Stroke and Flash Behavior

- 3 Yuval Ben Ami<sup>1</sup>, Ilan Koren<sup>1</sup>, Orit Altaratz<sup>1</sup> and Yoav Yair<sup>2</sup>
- 4 Department of Earth and Planetary Sciences, The Weizmann Institute of Science, Rehovot, 7610001, Israel.
- 5 <sup>2</sup>School of Sustainability, Reichman University, Herzliya, 4610101, Israel.

7 Correspondence to: Orit Altaratz (orit.altaratz@weizmann.ac.il)

9

11

8

6

#### Abstract

- 12 Lightning flashes play a key role in the global electrical circuit, serving as markers of deep convection and indicators of
- 13 climate variability. However, this field of research remains challenging due to the wide range of physical processes and
- 14 spatiotemporal scales involved.
- 15 This study utilizes the Lightning Differential Space (LDS), which maps lightning stroke intervals onto a parameter space
- defined by their temporal and spatial derivatives.
- 17 Using data from the Earth Networks Total Lightning Network (ENTLN), we analyze the Number Distribution LDS
- 18 clustering patterns across specific seasons in three climatically distinct regions: the Amazon, the Eastern Mediterranean
- 19 Sea, and the Great Plains in the US. The LDS reveals a robust clustering topography composed of "allowed"
- 20 and "forbidden" interval ranges, which are consistent across regions, while shifts in cluster position and properties reflect
- 21 the underlying regional meteorological conditions.
- 22 As an extension of the LDS framework, we introduce the Current Ratio LDS, a new diagnostic for identifying flash
- 23 initiation by mapping the ratio of peak currents between successive strokes into the LDS coordinates. This space reveals
- 24 a spatiotemporal structure that enables a clearer distinction between local and regional scales. It also reveals a distinct
- cluster, suggesting a possible teleconnection between remote strokes, spanning tens to hundreds of kilometers.
- 26 Together, the Number Distribution LDS and the novel Current Ratio LDS provide a scalable, data-driven framework for
- 27 analyzing and interpreting large datasets of CG lightning activity. This approach is suitable for comparing storm regions,
- validating lightning models, and enhancing early warning systems.

29





## 1. Introduction

- 31 Cloud-to-Ground (CG) lightning flashes play a significant role in the atmospheric global electric circuit (Siingh et al.,
- 32 2007), making it essential to understand their properties and driving mechanisms. In addition, studying CG flashes is
- important for improving safety measures, as they pose severe hazards to life and infrastructure (Yair, 2018).
- 34 Thunderclouds are the building blocks of deep cloud systems. The size of a single Cumulonimbus typically ranges
- between a few to a few tens of kilometers, depending on the season and location (Cotton and Heever, 2011). Its lightning
- 36 production rate varies between one flash every few seconds to one every few minutes, for a total duration ranging from a
- 37 few minutes up to ~1 h (Dwyer and Uman, 2014). The lightning production rate and the total duration of the
- thundercloud's electrical activity depend on dynamic and microphysical processes, such as the updraft's magnitude, the
- 39 depth of the mixed-phase region, and the fluxes of liquid water, graupel, and ice mass within the cloud (Deierling and
- 40 Petersen, 2008; Deierling et al., 2008). A major part of the CG flashes (mainly negative ones) consists of multi-stroke
- 41 flashes, transferring charge to the ground through several return strokes, some of which may follow different channels
- 42 that contact the ground within a radius of ~10 km (Dwyer and Uman, 2014). The gaps between the strokes are generally
- 43 a few tens of milliseconds, and a CG flash has a total duration is 0.5-1 seconds. Studies have statistically shown that the
- 44 first return stroke in a lightning flash generally has a stronger peak current than the subsequent strokes (Chowdhuri et al.,
- 45 2005; Poelman et al., 2013; Diendorfer et al., 2022). Positive CG flashes usually consist of a single return stroke and have
- a higher peak current compared to negative ones (Rakov, 2003).
- 47 Many previous studies have examined the spatiotemporal properties of strokes and flashes and their relation to the micro
- 48 and macrophysical properties of thunderclouds (e.g., Mattos and Machado, 2011; Strauss et al., 2013). These properties
- depend on geographic location, the season, and the type of convective system.
- 50 Observational studies also show that when thunderclouds cluster into an organized system, distinct spatial and temporal
- 51 lightning patterns emerge. For example, in the case of Mesoscale Convective Systems (MCS), this can include a high rate
- 52 of cloud-to-ground (CG) flashes, a large horizontal extent of flashes, a bipolar pattern of ground contact points, and other
- characteristics (MacGorman and Rust, 1998). On a larger scale, some studies suggest a coupling mechanism between
- 54 widely separated thunderclouds, leading to a synchronized lightning activity pattern (teleconnection; Mazur, 1982;
- 55 Vonnegut et al., 1985; Yair., et al 2006; 2009).
- 56 Due to the dependence on environmental conditions, investigating flash and stroke characteristics can greatly benefit from
- 57 large datasets. Lightning detection networks are valuable tools for this purpose, utilizing years of measurements collected
- over both land and ocean.
- With advancements in measurement technology and retrieval algorithms, there is growing interest in developing analysis
- 60 techniques that can extract new physical insights from existing long-term lightning network data. Here, we extend the
- 61 investigation of Ben Ami et al. (2022), who presented a unique differential space that reveals common properties of time
- and distance intervals between successive strokes, to provide insights into CG flash activity on both thundercloud and
- 63 cloud-system scales. Their work was focused on winter Cyprus-Lows in the Eastern Mediterranean, analyzing ~50,000
- 64 CG strokes that were measured by the Israel Lightning Location System (ILLS, Katz and Kalman, 2009), and introduced
- 65 the LDS as a novel data-driven diagnostic framework to differentiate between electrical events across a wide range of
- 66 spatial and temporal scales.
- 67 In the current study, we expand this investigation to three Regions Of Interest (ROI), representing different climatic
- 68 regimes, using CG data collected by a global lightning detection network with a larger dataset per region. In addition to





extending the Number Distribution LDS to new environments, a main goal of this work is to introduce the Current Ratio

LDS (see section 2.3) - a new diagnostic framework for identifying flash initiation intervals based on peak current
sequencing.

# 2. Data and Methods

#### 2.1. Regions and Seasons

The three ROIs are (a) the Amazon (0°-6°S; 66.6°W-59°W), representing the tropics (b) the Eastern Mediterranean Sea (31°N-35°N; 25°E-35.5°E), representing the sub-tropics and (c) the northern part of the US Great Plains (42°N-49°N; ~106°W-97°W), representing mid-latitudes (Fig. 1). These three ROIs were selected for three main reasons: (a) they represent three different climate regimes, (b) they experience intensive electrical activity during specific months (Cooper et al., 2019; Oda et al., 2022; Altaratz et al., 2003; Jiang et al., 2006; Kaplan et al., 2022), and (c) they are all characterized by flat terrain which is important for minimizing the effect of orographic convection on the analysis. Using large datasets, we analyze and compare the electrical activity in those three regions.

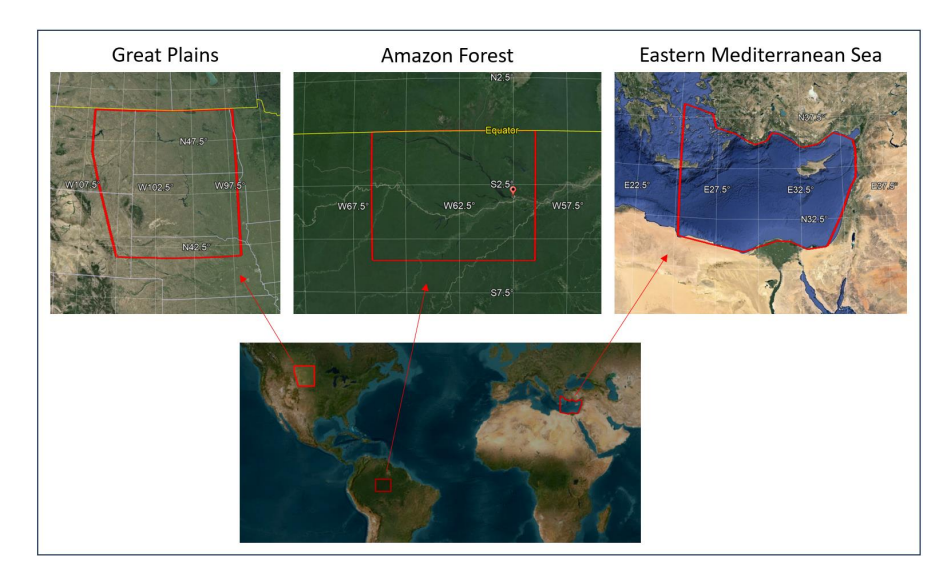


Figure 1: Maps marking the study regions (© Google Maps 2015). The Amazon is bounded between 0°-6°S and 66.6°W-59°W, the Great Plains at 42°N-49°N; ~106°W-97°W, and the Eastern Mediterranean Sea is approximately between 31°N-35°N; 25°E-5.5°E.

## 2.1.1 The Amazon (Sep.-Nov.)

During the wet season, lightning activity reaches its annual peak, as the Intertropical Convergence Zone migrates southward (Nobre et al., 2009), creating a belt of low pressure. At the same time, the upper levels are controlled by the Bolivian High (Molion, 1993). The convection is driven by local instability and moisture supplied by the forest (Wright et al., 2017). Additionally, low-level easterly winds transport humidity from the Ocean inland, all supporting the development of intense convection and electrical activity in the Amazon. Additional synoptic systems that support thunderstorm activity during the wet season include the South American Monsoon system (Williams et al., 2002) and the South Atlantic Convergence Zone, which is a quasi-stationary band of deep clouds that extends from the Amazon Basin southeastward (Carvalho et al., 2004).





## 2.1.2 The Eastern Mediterranean Sea (Oct.-Dec.)

The most intense electrical activity in this region occurs during the boreal autumn and winter, driven mainly by midlatitude cyclones. In these systems, continental cold air masses from Europe are advected toward the Mediterranean. As they propagate eastward, over the relatively warm sea, their moisture content increases, and they become unstable. The low-pressure center is usually located near Cyprus, commonly referred to as Cyprus Lows. Thunderclouds develop over the sea and near the coast, along cold fronts and post-frontal regions. A less frequent system is the Red Sea Trough (Ziv et al., 2005; Shalev et al., 2011), originating from the African monsoon over the Red Sea. When it is accompanied by an upper-level trough, it can support intense electrical activity over the Eastern Mediterranean Sea and neighboring countries, often leading to severe flooding.

## 2.1.3 The Northern Great Plains (Jun.-Aug.)

During this time of year, this region is part of the corridor for passing MCS, which are large clusters of thunderstorms (Tuttle and Davis, 2006). MCSs often develop or intensify during the night, while they develop along fronts (Ziegler and Rasmussen, 1998; Maddox et al., 1986) or drylines, which are the boundary between moist air from the Gulf of Mexico and dry air from the desert Southwest (Scaff et al., 2021). MCS can be sustained by a low-level jet as well, which peaks after sunset and drives a southerly wind that supplies warm and humid air from the Gulf of Mexico (Higgins et al., 1997).

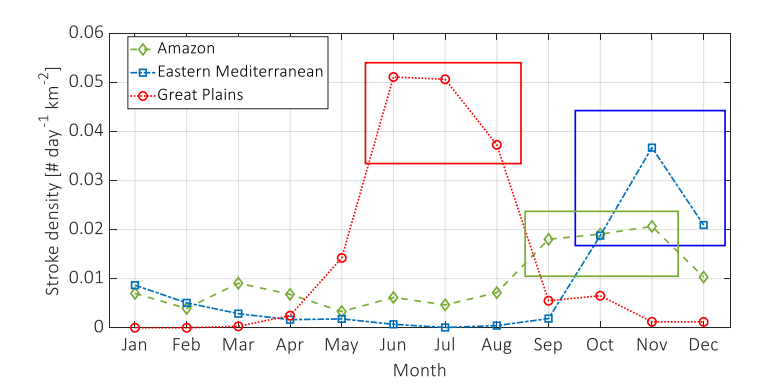


Figure 2: A histogram of the daily CG density (# day<sup>-1</sup>km<sup>-2</sup>) per month during 2020-2021. The selected months for analysis are indicated, based on the largest stroke density for each ROI.

# 2.2. Measurement System and Data

The CG stroke data used in this study were primarily retrieved by the ENTLN (Zhu et al., 2022), a global lightning detection network. This network is comprised of more than 1,500 wideband (1 Hz-12 MHz) sensors, deployed globally. Based on the detected electric field waveform and the time-of-arrival technique, the network estimates the pulse type (CG or intra-cloud; IC), ground contact point, time of impact, peak current, and polarity.

Based on analysis of rocket-triggered and natural flashes, the reported CG stroke detection efficiency and classification accuracy (estimated over the USA) are at least 96% and 86%, respectively. The median location error is 215 m and the absolute peak current error is 15%. A detailed description of the network performance can be found in Zhu et al. (2022).

In this study, we use CG stroke data. To minimize the impact of the interannual variability, we focus on a specific season for each ROI, selected based on the highest stroke density observed throughout the years (Fig. 2, Table 1). The total analyzed dataset includes 8,337,978 strokes, detected during 182 days in the Amazon, 118 days in the Eastern Mediterranean, and 175 days in the Great Plains, during 2020-2021.





To support and validate our ENTLN results, we use an additional CG dataset, measured by another lightning network, the Israeli Lightning Location System. At the time, the ILLS network included eight sensors, sensitive to the electric and/or magnetic field (Katz and Kalman, 2009). It detected 251,393 CGs during 265 stormy days with diverse synoptic conditions, from Oct. to Dec., from 2004 to 2008, and 2010. Our ILLS dataset does not overlap with the ENTLN period (2020–2021), but it covers similar months along the year and hence a similar type of synoptic systems, and can be used for validation. Due to the detection limits of the ILLS, the validation of the ENTLN analysis against the ILLS data was done in a different area that covers 250 km from the network center over the Eastern Mediterranean Sea and the adjacent land (Fig. S1). This ILLS data was used in the previous work by Ben Ami et al (2022).

Table 1. Season, study area [km²], total number of analyzed days (with detected CG flashes), total number of analyzed hours, total number of detected CG strokes, number of strokes in clusters A, B+C, and D, and estimated flash density per ROI. (\* Estimated from the ratio between the number of intervals B+C+1, to the area, and the number of days).

	Amazon	Eastern Mediterranean	Great Plains	Total
Season	SepNov.	OctNov.	JunAug.	-
Area [km <sup>-2</sup> ]	563,270	566,010	562,730	1,692,010
# of days	182	118	175	475
Number of hours [#]	3,740	1,979	2,854	8,573
Number of CGs	1,974,302	1,790,482	4,573,194	8,337,978
Number of intervals in A [#]	674,538	863,374	869,395	2,407,307
Number of intervals in B+C [#]	1,282,533	894,543	3,642,374	5,819,450
Number of intervals in D [#]	17,230	32,564	61,424	111,221
Flash density [# km <sup>-2</sup> day <sup>-1</sup> ]*	0.013	0.013	0.037	-

# 

#### 2.3. Method

The CG stroke data was sorted by the time of ground impact. Next, the time (dT) and distance (dR) intervals between consecutive strokes were calculated by subtracting the detection times and computing the distance between the geographical coordinates of each stroke pair. The number of events per interval range was projected onto a two-dimensional differential space, defined by dR and dT, termed the Lighting Differential Space (LDS; this representation is referred to as the Number Distribution LDS). The density-based classification and visualization method, introduced by Ben Ami et al. (2022), requires no preprocessing of the data or the usage of machine learning algorithms, and offers an efficient way to extract statistically meaningful patterns from large lightning datasets. On one hand, it eliminates information on the stroke ground contact point and absolute time of incidence, and on the other, it clusters pairs of strokes with similar time and space interval properties.

To identify interval ranges with a higher likelihood of containing the initial stroke in a flash, we analyzed the peak currents of consecutive strokes by projecting the ratio of the absolute current value (polarity agnostic) between the  $2^{nd}$  and  $1^{st}$  strokes in each pair onto the LDS coordinate system. This approach introduces the Current Ratio LDS. As we anticipate that the peak currents of strokes will decrease sequentially within a flash (Chowdhuri et al., 2005), the current ratio LDS is used to identify intervals that are more likely to contain the initial stroke in a flash.

#### 3. Results and Discussion

The number distribution LDS (Fig. 3a-c) clusters stroke intervals with similar dR and dT into "allowed" and "forbidden" interval ranges. Two main clusters with a high probability of occurrence are indicated. Zero and low count values reveal





the forbidden ranges of dR and dT intervals. This general clustering topography is consistently observed across all three ROIs. However, shifts in cluster position and variations in their characteristics reflect underlying meteorological differences among the three regions.

The first cluster, marked as A, is characterized by short intervals between successive strokes both in time and space. For all the ROIs, most of the events occur in dT < 0.5 sec, and it is limited to dR of a few km and up to a few tens of km. The second cluster, marked as C, extends over longer dTs and larger dRs. Cluster A represents time and space intervals between strokes in multiple-stroke flashes (multiplicity > 1), as it fits the characteristics of consecutive CG strokes within a flash (Poelman, 2021; Wu et al., 2020). In contrast, cluster C groups the intervals between the last stroke in one flash and the initial stroke in the next flash, initiated by a distant thundercloud, in agreement with Ben Ami et al. (2022). In the case of a MCSs', which often spans over hundreds of kilometers, it could be initiated by a distant convective cell in the same wide-scale system. Note that the position of cluster C is scale-dependent, and it is linked to the ROI's area. Nevertheless, we chose the area of the ROIs to be on the order of 500,000 km² (Table 1) to cover a synoptic scale, hence cluster C location indicates a typical scale of distances between electrical events at a synoptic (meso) scale.

In addition to two dominant clusters, we also identify a ridge-like weak cluster, called here B, representing stroke intervals between consecutive flashes within a thundercloud. Unlike in Ben Ami et al. (2022), who analyzed a smaller ILLS dataset, B has no clear centers across all ROIs. This is due to the larger dataset of the ENTLN analyzed here and the inclusion of various synoptic conditions. The presence of B in the ENTLN data is illustrated in the supplementary section (Fig. S2) for a smaller dataset. To further validate our findings, we analyzed the ILLS data for the Eastern Mediterranean (Fig. S1). The results indicate a similar manifestation of B, appearing as a ridge in the number distribution LDS, without a distinct center (see Fig. S3).

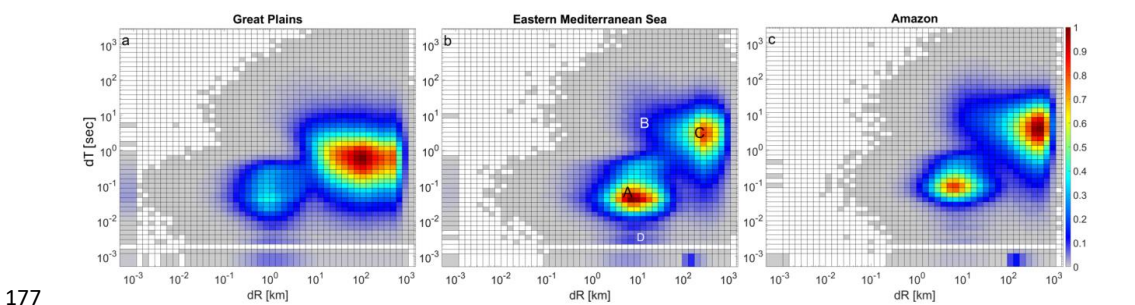


Figure 3: Number distribution LDS: PDF of the dR and dT intervals between consecutive strokes, normalized by the maximum number of counts, for (a) the Great Plains, (b) Eastern Mediterranean, and (c) the Amazon. The locations of clusters A-D are illustrated in panel b. Intervals with PDF < 0.025 are marked in gray.

Figure 4 shows the projection of the PDFs (from Fig. 3) onto the dR (X) and dT (Y) axes. The projection on the dT axis (Fig. 4b) clarifies that in the Great Plains, there is no temporal separation between clusters A and C, that is, between events occurring at the cloud scale and at the cloud system scale. This contrasts with the well-defined temporal separation between clusters A and C observed in the other two regions, the Eastern Mediterranean and the Amazon. This, and the relatively shorter dTs of cluster C (between ~0.1-2.4sec), are a result of the high flash density in the Great Plains region





(0.037 km<sup>-2</sup> day<sup>-1</sup>, see Table 1). This density is about three times greater than the flash density in the Eastern Mediterranean and the Amazon (0.013 km<sup>-2</sup> day<sup>-1</sup>, Table 1). This finding is supported by Kastman et al. (2017), who report a high CG flash rate for a certain type of MCSs passing over the Great Plains during this season. The elevated flash density in this region is likely related to the frequent occurrence of MCSs and long-lived mesoscale systems, which are characterized by high frequency of electrical events and hence shorter intervals between flashes, thereby shifting cluster C toward shorter dTs.

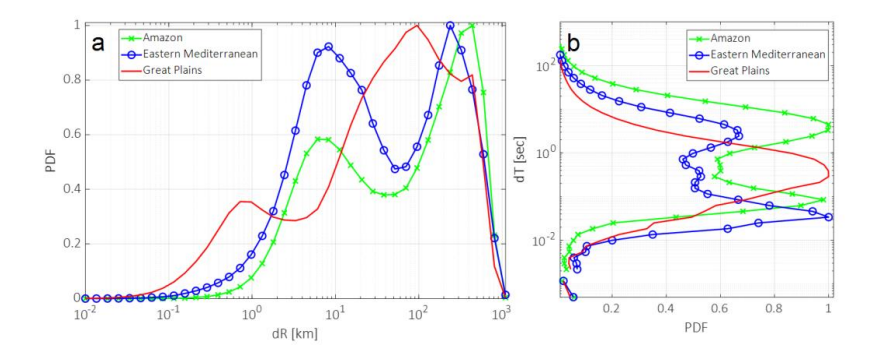


Figure 4: Projections of the number distributions LDS in Fig.1 on the dR (a) and dT (b) axes.

Additional differences between the ROIs can be recognized when examining the clusters' location along the dR axis. While in the Amazon and the Eastern Mediterranean cluster C is centered around 250-400 km, in the Great Plains it is located at a shorter distance of ~100 km (Fig. 3 and Fig. 4a). This indicates a smaller characteristic distance, at the cloud-system scale, between electrical events in the Great Plains. In addition, the characteristic dR of cluster A is different: it is located around 7 km in the Eastern Mediterranean and the Amazon and around ~1 km in the Great Plains, suggesting a smaller, denser ground impact radius of strokes within a flash. Poelman et al. (2021) observed a similar tendency for shorter distances between ground strike points within a flash over the US (Florida) when examined against a few other regions in Europe, Brazil, and South Africa. Their reported median value of 1.3 km is comparable to our findings for the Great Plains. Nevertheless, we cannot rule out that this is a manifestation of smaller location errors over the Great Plains due to the higher density of ENTLN sensors in the US. The denser sensor coverage in this region results in better detection accuracy and improved spatial resolution, which could contribute to the shorter dR values observed in Cluster A (Fig. 3-4).

Another analysis we performed to study stroke characteristics in the different ROIs is the projection of consecutive strokes' peak current ratio on the LDS coordinate system (Fig. 5). That is, the ratio between the absolute current of the 2<sup>nd</sup> and the 1<sup>st</sup> stroke in each of the pairs. Given that statistically the peak current of CG strokes decreases monotonically with their order within a flash, we identified interval ranges that are more likely to represent the initial stroke in a flash (see schematic illustration in Fig. S4). Complementary to the number distribution LDS in Fig. 3, we find that the current ratio LDS functions like a partitioning algorithm rather than a clustering method. It separates the space into dR and dT interval ranges, where the current amplitude of the succeeding stroke is statistically larger (reddish) or smaller (bluish) than that of the preceding one. In agreement with the interpretation of the clusters on the number distribution LDS, in clusters B and C, the 2<sup>nd</sup> stroke in a pair is more likely to have a stronger peak current (reddish), hence assumed to be the

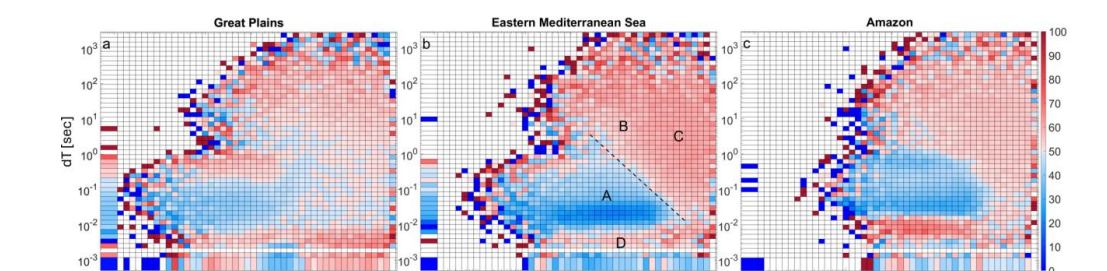




initial stroke in a new, different flash. Accordingly, in cluster *A*, representing consecutive strokes in multiple-stroke CG flashes, the 2<sup>nd</sup> stroke in a pair is more likely to have a smaller peak current (bluish).

This clear and sharp separation into distinct red and blue regions on the current ratio LDS is consistent and repeatable across the three ROIs, although it is less distinct in the Great Plains. A similar separation between initial and successive strokes within a flash, clearly separated into red and blue zones, can be seen in the current ratio LDS produced from the ILLS network data (Fig. S5), which was used as a validation dataset. The agreement between the two independent detection systems supports the robustness of our findings, that this is a consistent property of lightning discharge sequences in thunderstorms.

The diagonal borderline between events is illustrated in Fig. 5b. It is not a strict physical boundary but a statistical partition that reflects the dominant stroke-pair dynamics: initial strokes (reddish) vs. inter-flash strokes (bluish). It indicates that the shorter the distance between strokes, the longer the delay to the next flash. Focusing on time scales of a few seconds and distances of a few tens of km, Zoghzoghy et al. (2013) reported a similar inverse relation between the distance and the time to the next stroke. Here, we demonstrate that this relationship may also apply on a sub-second timescale and across tens of kilometers.



10<sup>3</sup>

Figure 5: Current ratio (between the absolute current of 2<sup>nd</sup> and 1<sup>st</sup> strokes in each pair) LDS for (a) the Great Plains, (b) Eastern Mediterranean, and (c) the Amazon: The percent of pairs with stronger successive stroke peak current (2<sup>nd</sup> in pair). Reddish intervals indicate a stronger amplitude of the 2<sup>nd</sup> stroke in more than 50% of the pairs, while the bluish intervals show the opposite. The location of clusters A-D is illustrated on panel b. The borderline between the main reddish and bluish regions is illustrated by the dashed line on panel b.

10<sup>1</sup>

An interesting and new feature, that appears in the current ratio LDS of the three ROIs', is cluster D (marked in Fig. 5b). This cluster is characterized by very short dTs (on the order of <0.02 sec), which are shorter than the characteristic dT of cluster A, and a very wide range of dRs, ranging from hundreds of meters to hundreds of kilometers. Containing less than 2% of the data, cluster D is not distinct when examining the numbers of events on the LDS (Fig. 3). Its topography becomes visible only when examining the current ratio LDS (Fig. 5).

The validation analysis, similar to the main analysis but using the ILLS network data, reveals a similar D cluster (Fig S5). It supports the robustness of this finding and eliminates the possibility that D is an artifact of the ENTLN retrieval algorithm.

# https://doi.org/10.5194/egusphere-2025-4052 Preprint. Discussion started: 22 October 2025 © Author(s) 2025. CC BY 4.0 License.





The high percentage of a stronger peak current of the 2<sup>nd</sup> stroke in a pair in cluster D (similar to clusters B and C) indicates that they are probably the initial strokes in flashes. However, cluster D spans a wide range of distances (dRs). For short distances, up to ten or a few tens of km, it may indicate electrical events within the same thundercloud. It appears when a consecutive stroke in a multiple-stroke flash is more intense than the previous one, as expected for ~30% of the flashes (Diendorfer et al., 2022). In that respect, it is interesting to see the clustering of such events at shorter dTs than the typical inter-stroke dT intervals in cluster A. The part of cluster D that pertains to much longer dRs indicates electrical events of two strokes that take place nearly simultaneously but at locations that are tens and hundreds of km away. Several studies have suggested a similar temporal sequence of remote flashes. Although the exact mechanism is yet to be elucidated, several processes have been proposed, suggesting that their nearly simultaneous occurrence is not a pure coincidence and that there is a physical mechanism that ties these remote strokes together. Füllekrug (1995), Ondrášková et al. (2008), and Yair et al. (2006) have suggested triggering by the Schumann resonance. Later, Yair et al. (2009) proposed a theoretical model by which a lightning flash may enhance the electric field in neighboring cells, as a function of the distance between them, potentially triggering a near-simultaneously flash in a remote (mature) thundercloud. Here, using only data from a lightning location network, we cannot confirm nor rule out those lightning-triggering mechanisms that may explain the part of cluster D with longer dRs.

#### 4. Summary

- This study focuses on the parameters of CG flashes within individual thunderclouds and cloud systems. We analyzed the number of stroke intervals and the peak current ratio between successive strokes in the Lighting Differential Space (LDS) domain (Ben Ami et al., 2022). Three distinct climatic regions were examined: the Amazon, the Eastern Mediterranean Sea, and the Great Plains in the USA.
- By clustering similar events, the Number Distribution LDS enables differentiation between electrical events on the scale of a single thundercloud versus those of a larger cloud system. The identified clusters represent initial strokes in individual thunderclouds (ridge B), in a cloud system (cluster C), and successive strokes in multi-stroke flashes (cluster A).
- The Current Ratio LDS emerges as a new key diagnostic tool. It sharply and consistently discriminates between interval ranges that are more likely to contain initial strokes in flashes and those that are not. A fourth cluster (D) indicates occurrences of successive strokes striking the ground tens to hundreds of kilometers apart, yet within just a few milliseconds of each other, suggesting possible long-range interaction between thunderstorms.
- Overall, the LDS provides a scalable and objective framework for analyzing big datasets of stroke row data and interpreting multiscale lightning activity. It reveals coherent spatiotemporal patterns and regional similarities in flash behavior. This method applies to a range of operational applications, including comparative analysis of storm regions, lightning model validation, and the enhancement of early warning systems.





281	Data availability
282 283 284	The lightning stroke data used in this study were obtained from commercial sources under license and are not publicly available. Access to these data is restricted by data use agreements with the Earth Networks Total Lightning Network (ENTLN) and the Israel Lightning Location System (ILLS).
285	Author contribution
286	Conceptualization: IK, YBA and OA. Analysis: YBA. Writing & review: YBA, OA, IK, and YY.
287	Competing interests
288	The contact author has declared that none of the authors has any competing interests.
289	Disclaimer
290 291	The views and conclusions expressed in this article are solely those of the authors and do not necessarily reflect the views of the data providers. The authors have no financial or commercial interest in the data sources used in this study.
292	Acknowledgemnt
293	N\A
294	Financial support
295 296 297	This project has received funding from the European Research Council (ERC) under the European Union's Horizon 2020 research and innovation programme (grant agreement No 810370), and YY was supported by the Israeli Science Foundation grant ISF 1848/20.
298	Review statement
299	This paper is currently under review for the journal Atmospheric Measurement Techniques.
300	
301	
302	





#### References

- Altaratz, O., Levin, Z., Yair, Y., and Ziv, B.: Lightning activity over land and sea on the eastern coast of the
   Mediterranean, Monthly Weather Review 131, no. 9, 2060-2070, https://doi.org/10.1175/1520-0493(2003)131<2060:LAOLAS>2.0.CO;2, 2003.
- Ben Ami, Y., Altaratz, O., Koren, I., and Yair, Y.: Allowed and forbidden zones in a Lightning-strokes spatio temporal differential space, Environmental Research Communications, 4(3), p.031003, DOI 10.1088/2515 7620/ac5ec2, 2022.
- Carvalho, L.M., Jones, C. and Liebmann, B: The South Atlantic convergence zone: Intensity, form, persistence,
   and relationships with intraseasonal to interannual activity and extreme rainfall, Journal of Climate, 17(1), pp.88 108., https://doi.org/10.1175/1520-0442(2004)017%3C0088:TSACZI%3E2.0.CO;2, 2004.
- Chowdhuri, P., Anderson, J.G., Chisholm, W.A., Field, T.E., Ishii, M., Martinez, J.A., Marz, M.B., McDaniel,
   J., McDermott, T.E., Mousa, A.M., and Narita, T.: Parameters of lightning strokes: A review. IEEE Transactions
   on Power Delivery, 20(1), pp.346-358, doi: 10.1109/TPWRD.2004.835039, 2005.
- Cooper, M.A., and Holle, R.L.: Global lightning distribution. Reducing Lightning Injuries Worldwide, pp.107 114, <a href="https://doi.org/10.1109/TPWRD.2004.835039">https://doi.org/10.1109/TPWRD.2004.835039</a>, 2019.
- 6. Cotton, W.R., Bryan, G., and van den Heever, S.C.: Cumulonimbus clouds and severe convective storms, In International geophysics (Vol. 99, pp. 315-454), Academic Press, <a href="https://doi.org/10.1016/S0074-320">https://doi.org/10.1016/S0074-320</a> 6142(10)09914-6, 2011.
- 7. Deierling, W., and Petersen, W.A.: Total lightning activity as an indicator of updraft characteristics, Journal of Geophysical Research: Atmospheres, 113(D16), https://doi.org/10.1029/2007JD009598, 2008.
- Deierling, W., Petersen, W.A., Latham, J., Ellis, S., and Christian, H.J.: The relationship between lightning
   activity and ice fluxes in thunderstorms, Journal of Geophysical Research, Atmospheres, 113(D15),
   <a href="https://doi.org/10.1029/2007JD009700">https://doi.org/10.1029/2007JD009700</a>, 2008.
- Diendorfer, G., Bologna, F.F., and Engelbrecht, C.S.: A review of the relationship between peak currents of the
   first and subsequent strokes in the same flash, In 2022 36th International Conference on Lightning Protection
   (ICLP) (pp. 10-13), IEEE, <a href="https://doi.org/10.1109/ICLP56858.2022.9942502">https://doi.org/10.1109/ICLP56858.2022.9942502</a>, 2022.
- 329 10. Dwyer, J.R., and Uman, M.A.: The physics of lightning, Physics Reports, 534(4), pp.147-241, 2014.
- Füllekrug, M.: Schumann resonances in magnetic field components, Journal of Atmospheric and Terrestrial
   Physics, 57(5), pp.479-484, <a href="https://doi.org/10.1016/0021-9169(94)00075-Y">https://doi.org/10.1016/0021-9169(94)00075-Y</a>, 1995.
- Higgins, R.W., Yao, Y., Yarosh, E.S., Janowiak, J.E., and Mo, K.C.: Influence of the Great Plains low-level jet
   on summertime precipitation and moisture transport over the central United States, Journal of Climate, 10(3),
   pp.481-507, <a href="https://doi.org/10.1175/1520-0442(1997)010%3C0481:IOTGPL%3E2.0.CO;2">https://doi.org/10.1175/1520-0442(1997)010%3C0481:IOTGPL%3E2.0.CO;2</a>, 1997.
- 13. Kaplan, J.O., and Lau, K.H.K.,: World wide lightning location network (WWLLN) global lightning climatology
   336 (WGLC) and time series, 2022 update, Earth System Science Data, 14(12), pp.5665-5670,
   337 <a href="https://doi.org/10.5281/zenodo.6007052">https://doi.org/10.5281/zenodo.6007052</a>, 2022.





- 14. Kastman, J.S., Market, P.S., Fox, N.I., Foscato, A.L., and Lupo, A.R.: Lightning and rainfall characteristics in elevated vs. surface based convection in the midwest that produce heavy rainfall, Atmosphere, 8(2), p.36, https://doi.org/10.3390/atmos8020036, 2017.
- 15. Katz, E. and Kalman, G.: The impact of environmental and geographical conditions on lightning parameters
   derived from lightning location system in Israel, In Proceeding of the 10<sup>th</sup> International Symposium on Lightning
   Protection, Curitiba, Brazil, November (pp. 9-13), 2009.
- 16. MacGorman, D.R., and Rust, W.D.: The electrical nature of storms, Oxford University Press, USA, 1998.
- Maddox, R.A., Howard, K.W., Bartels, D.L., and Rodgers, D.M.: Mesoscale convective complexes in the middle
   latitudes, In Mesoscale meteorology and forecasting (pp. 390-413), Boston, MA: American Meteorological
   Society, 1986.
- Mattos, E.V., and Machado, L.A.: Cloud-to-ground lightning and Mesoscale Convective Systems, Atmospheric
   Research, 99(3-4), pp.377-390, <a href="https://doi.org/10.1016/j.atmosres.2010.11.007">https://doi.org/10.1016/j.atmosres.2010.11.007</a>, 2011.
- 350 19. Mazur, V:. Associated lightning discharges, Geophysical Research Letters, 9(11), pp.1227-1230,
   351 <a href="https://doi.org/10.1029/GL009i011p01227">https://doi.org/10.1029/GL009i011p01227</a>, 1982.
- 352 20. Molion, L.C.B.: Amazonia rainfall and its variability, Hydrology and water management in the humid tropics,
   353 Hufschmidt, M.M., Gladwell, J.S., Eds., pp.99-111, 1993.
- Nobre, C.A., Obregón, G.O., Marengo, J.A., Fu, R., and Poveda, G.: Characteristics of Amazonian climate: main
   features, Amazonia and global change, 186, pp.149-162, 2009.
- Oda, P.S., Enoré, D.P., Mattos, E.V., Gonçalves, W.A., and Albrecht, R.I.: An initial assessment of the
   distribution of total Flash Rate Density (FRD) in Brazil from GOES-16 Geostationary Lightning Mapper (GLM)
   observations, Atmospheric Research, 270, p.106081, https://doi.org/10.1016/j.atmosres.2022.106081, 2022.
- 23. Ondrášková, A., Bór, J., Kostecký, P., and Rosenberg, L.: Peculiar transient events in the Schumann resonance
   band and their possible explanation, Journal of atmospheric and solar-terrestrial physics, 70(6), pp.937-946,
   https://doi.org/10.1016/j.jastp.2007.04.013, 2008.
- 24. Poelman, D.R., Schulz, W., Pedeboy, S., Hill, D., Saba, M., Hunt, H., Schwalt, L., Vergeiner, C., Mata, C.,
   Schumann, C., and Warner, T.: Global ground strike point characteristics in negative downward lightning
   flashes-Part 1: Observations, Natural Hazards and Earth System Sciences Discussions, 2021, pp.1-17,
   https://doi.org/10.5194/nhess-21-1909-2021, 2021.
- Rakov, V.A., A review of positive and bipolar lightning discharges, Bulletin of the American Meteorological
   Society, 84(6), pp.767-776, <a href="https://doi.org/10.1175/BAMS-84-6-767">https://doi.org/10.1175/BAMS-84-6-767</a>, 2003.
- Scaff, L., Prein, A.F., Li, Y., Clark, A.J., Krogh, S.A., Taylor, N., Liu, C., Rasmussen, R.M., Ikeda, K., and Li,
   Z., Dryline characteristics in North America's historical and future climates, Climate Dynamics, 57(7), pp.2171 2188, <a href="https://doi.org/10.1007/s00382-021-05862-1">https://doi.org/10.1007/s00382-021-05862-1</a>, 2021.





- Shalev, S., Saaroni, H., Izsak, T., Yair, Y., and Ziv, B.: The spatio-temporal distribution of lightning over Israel
   and the neighboring area and its relation to regional synoptic systems, Natural Hazards and Earth System
   Sciences, 11(8), pp.2125-2135, https://doi.org/10.5194/nhess-11-2125-2011, 2011.
- Siingh, D., Gopalakrishnan, V., Singh, R.P., Kamra, A.K., Singh, S., Pant, V., Singh, R., and Singh, A.K.: The
   atmospheric global electric circuit: an overview, Atmospheric Research, 84(2), pp.91-110,
   <a href="https://doi.org/10.1016/j.atmosres.2006.05.005">https://doi.org/10.1016/j.atmosres.2006.05.005</a>, 2007.
- Strauss, C., Rosa, M.B. and Stephany, S.: Spatio-temporal clustering and density estimation of lightning data for
   the tracking of convective events, Atmospheric Research, 134, pp.87-9,
   https://doi.org/10.1016/j.atmosres.2013.07.008, 2013.
- 30. Tuttle, J.D. and Davis, C.A.: Corridors of warm season precipitation in the central United States, Monthly Weather Review, 134(9), pp.2297-2317, <a href="https://doi.org/10.1175/MWR3188.1">https://doi.org/10.1175/MWR3188.1</a>, 2006.
- 38. Vonnegut, B., Vaughan Jr, O.H., Brook, M., and Krehbiel, P.: Mesoscale observations of lightning from space shuttle, Bulletin of the American Meteorological Society, 66(1), pp.20-29, <a href="https://doi.org/10.1175/1520-0477(1985)066%3C0020:MOOLFS%3E2.0.CO;2">https://doi.org/10.1175/1520-0477(1985)066%3C0020:MOOLFS%3E2.0.CO;2</a>, 1985.
- 32. Williams, E., Rosenfeld, D., Madden, N., Gerlach, J., Gears, N., Atkinson, L., Dunnemann, N., Frostrom, G.,
   386 Antonio, M., Biazon, B., and Camargo, R.Contrasting convective regimes over the Amazon: Implications for
   387 cloud electrification, Journal of Geophysical Research: Atmospheres, 107(D20), pp.LBA-50,
   388 <a href="https://doi.org/10.1029/2001JD000380">https://doi.org/10.1029/2001JD000380</a>, 2002.
- 33. Wright, J.S., Fu, R., Worden, J.R., Chakraborty, S., Clinton, N.E., Risi, C., Sun, Y., and Yin, L.. Rainforest-initiated wet season onset over the southern Amazon, Proceedings of the National Academy of Sciences, 114(32), pp.8481-8486, https://doi.org/10.1073/pnas.1621516114, 2017.
- 34. Wu, T., Wang, D., and Takagi, N.: Multiple-stroke positive cloud-to-ground lightning observed by the FALMA
   in winter thunderstorms in Japan, Journal of Geophysical Research: Atmospheres, 125(20), p.e2020JD033039,
   <a href="https://doi.org/10.1029/2020JD033039">https://doi.org/10.1029/2020JD033039</a>, 2020.
- 35. Yair, Y., Aviv, R., Ravid, G., Yaniv, R., Ziv, B., and Price, C.: Evidence for synchronicity of lightning activity
   in networks of spatially remote thunderstorms, Journal of atmospheric and solar-terrestrial physics, 68(12),
   pp.1401-1415, <a href="https://doi.org/10.1016/j.jastp.2006.05.012">https://doi.org/10.1016/j.jastp.2006.05.012</a>, 2006.
- 398 36. Yair, Y.Y., Aviv, R., and Ravid, G.: Clustering and synchronization of lightning flashes in adjacent thunderstorm cells from lightning location networks data, Journal of Geophysical Research: Atmospheres, 114(D9), <a href="https://doi.org/10.1029/2008JD010738">https://doi.org/10.1029/2008JD010738</a>, 2009.
- 37. Yair, Y.: Lightning hazards to human societies in a changing climate, Environmental research letters, 13(12),
   p.123002, DOI 10.1088/1748-9326/aaea86, 2018.
- 38. Zhu, Y., Stock, M., Lapierre, J., and DiGangi, E.: Upgrades of the Earth networks total lightning network in 2021, Remote sensing, 14(9), p.2209, <a href="https://doi.org/10.3390/rs14092209">https://doi.org/10.3390/rs14092209</a>, 2022.





405	39. Ziegler, C.L., and Rasmussen, E.N.: The initiation of moist convection at the dryline: forecasting issues from a
406	case study perspective, Weather and forecasting, 13(4), pp.1106-1131, https://doi.org/10.1175/1520-
407	<u>0434(1998)013%3C1106:TIOMCA%3E2.0.CO;2</u> , 1998.
408	40. Ziv, B., Dayan, U., and Sharon, D.: A mid-winter, tropical extreme flood-producing storm in southern Israel:
409	synoptic scale analysis, Meteorology and Atmospheric Physics, 88, pp.53-63, https://doi.org/10.1007/s00703-
410	<u>003-0054-7,</u> 2005.
411	41. Zoghzoghy, F.G., Cohen, M.B., Said, R.K., and Inan, U.S.: Statistical patterns in the location of natural lightning,
412	Journal of Geophysical Research: Atmospheres, 118(2), pp.787-796, https://doi.org/10.1002/jgrd.50107, 2013.